Materials and Methods: Clinical data from 469 inoperable NSCLC patients, treated with curative intent with chemoradiation (CRT) or radiotherapy (RT) alone were collected. The esophagus was delineated using the external esophageal contour from the cricoid cartilage to the GE junction. A Bayesian network model was developed to predict severe acute dysphagia (≥ Grade 3 according to the CTCAEv3.0). Data was weighted in proportion to how recent the RT took place. The model utilized gender, WHO performance status, mean esophageal dose, maximum esophageal dose and overall treatment time to make predictions. The model was trained on data from 363 patients. The model's performance was assessed on data from the 106 most recently treated patients and expressed as the Area Under the Curve (AUC) of the Receiver Operating Characteristic (ROC). The maximum value of the AUC is 1.0; indicating a perfect prediction model. A value of 0.5 indicates that patients are correctly classified in 50% of the cases, e.g., as good as chance. Comparison of ROC curves was done using the method described in Hanley and McNeil (1983).

Results: Fifty-one patients (11%) developed acute severe dysphagia. The model was validated on a dataset of 106 recently treated patients. The AUC of the model that weights data based on its novelty was 0.69 (95%CI, 0.59–0.77) *versus* an AUC of 0.64 (95%CI, 0.54–0.73) for the model that treats all data with equal importance. The ROC curves are significantly different (P < 0.05).

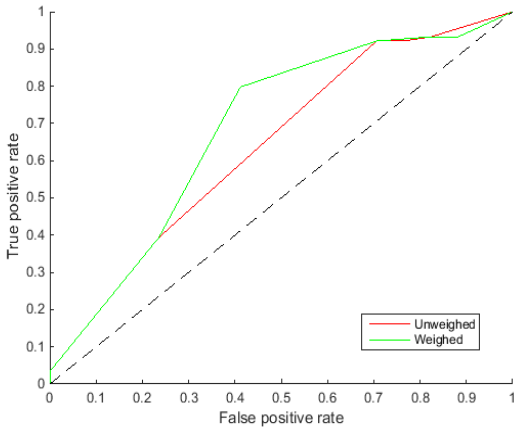

Conclusions: An increase in classification performance is observed by weighting data in proportion to how recent the treatment has occurred. The Bayesian network could be used in clinical practice to more accurately predict patients at high risk of developing acute dysphagia. Furthermore, this study shows the potential of rapid learning health care systems to develop and update prediction models for personalized treatment of cancer patients.

PO-0904

Minimizing late effects for patients with mediastinal Hodgkin lymphoma: deep inspiration breath-hold and/or IMRT?

M. Aznar[1], M.V. Maraldo[1], D.A. Schut[1], M. Lundemann[1], N.P. Brodin[2], I.R. Vogelius[1], A.K. Berthelsen[1], L. Specht[1], P.M. Petersen[1]

[1]Rigshospitalet, Section for Radiotherapy Department of Oncology 3993, Copenhagen, Denmark
[2]Albert Einstein College of Medicine of Yeshiva University, Institute of Onco-Physics, Copenhagen, Denmark

Purpose/Objective: Hodgkin Lymphoma (HL) survivors have an increased risk of cardiovascular disease (CVD), lung cancer and breast cancer. We estimated the risk of developing CVD and secondary lung, breast, and thyroid cancer after radiotherapy (RT) delivered with deep inspiration breath-hold (DIBH) compared to free-breathing (FB) using 3D conformal RT (3DCRT) and intensity modulated RT (IMRT). The aim of this study was to determine which treatment modality best reduced the combined risk of life-threatening late effects in patients with mediastinal HL.

Materials and Methods: Twenty two patients with early stage, mediastinal HL were eligible for the study and underwent a pre-chemotherapy PET/CT-scan in DIBH and in FB as well as a post-chemotherapy CT-scan in DIBH and in FB. All treatment plans delivered 30.6 Gy to initially involved nodes using either 3DCRT or IMRT on both the DIBH- and FB-sets, with equal target coverage requirements. We reported the estimated dose to the heart, lung, female breasts, and thyroid as well as the heterogeneity index (HI=$Dmax_{PTV}$/(prescription dose)) and conformity index (CI= $V95\%_{body}$/$Volume_{PTV}$) for each plan. The excess risks were calculated using dose-response relationships from large series of HL survivors with long-term follow-up (CD, lung cancer and breast cancer) and from the Childhood Cancer Survivor Study (thyroid cancer). The 'life-years lost' (LYL) measure was used compare the risks of late effects on a common scale (considering age-at-exposure, life-expectancy, and prognosis of the different late effects). Results were analyzed using a repeated measures analysis of variance (rANOVA) with treatment technique as a categorical variable (3D-DIBH, IMRT-DIBH, 3D-FB or IMRT-FB).

Results: DIBH lowered the dose to heart and lung regardless of delivery technique ($p<0.001$), cf. figure 1. The mean breast dose was increased with IMRT regardless of breathing technique. There was no difference in HI between the 4 categories of plans ($p=0.3$), whereas IMRT plans were consistently more conformal than 3DCRT with a median CI of 2.5, 2.7, 1.2, and 1.2 for 3D-FB, 3D-DIBH, IMRT-FB, and IMRT-DIBH, respectively. The overall lowest risk estimates for CVD and lung cancer were seen with IMRT-DIBH and for breast cancer with 3D-DIBH (see table 1). DIBH provided the lowest total LYL (with a range of 0.1-1.2 years for 3D-DIBH and 0.1-1.3 for IMRT-DIBH) and FB the highest (0.1-1.7 and 0.1-1.8 for 3D-FB and IMRT-FB respectively). For both DIBH and FB, 3DCRT vs. IMRT were not significantly different in *post hoc* tests for LYL.

Table 1: Excess relative risk estimates for the 22 patients with early stage mediastinal Hodgkin lymphoma in DIBH or FB delivered with 3DCRT or IMRT

	3D FB		IMRT FB		3D DIBH		IMRT DIBH		
	Median	Range	Median	Range	Median	Range	Median	Range	all
Risk Estimates (%)									
Myocardial infarction	4.9	0-19.4	4.5	0-13.1	2.9	0-17.5	2.1	0-11.1	<0.001
Thyroid cancer	<0.0001	0-0	<0.0001	0-0	<0.0001	0-0	<0.0001	0-0	N/A
Lung cancer	4.6	0.5-10.0	4.5	0.8-9.0	3.7	0.6-7.2	3.7	0.7-6.6	<0.001
Breast cancer	2.1	0.1-10.3	3.8	0.1-13.8	3.1	0.1-8.6	4.5	0.3-11.9	<0.001
Life Years Lost (years)	0.7	0.1-1.8	0.6	0.1-1.7	0.6	0.1-1.2	0.5	0.1-1.3	<0.001

Figure 1: mean estimated dose to OARs according to delivery technique

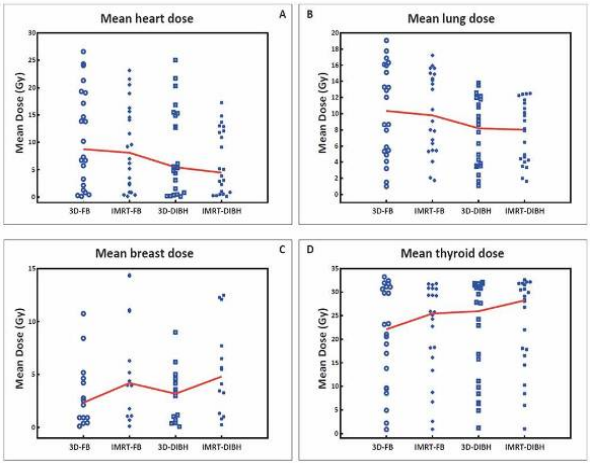

Conclusions: DIBH lowered the estimated dose to heart and lung while IMRT increased the mean breast dose regardless of breathing technique. In average, LYL was lowest with DIBH and highest with FB. Overall in this cohort, 3D-DIBH resulted in the lowest estimated doses life-time excess risks, though combining IMRT and DIBH could be beneficial for a sub-group of patients.

PO-0905

An individualised TCP model for radiotherapy of prostate cancer based on apparent diffusion coefficient maps

O. Carares-Magaz[1], U. Van der Heide[2], L. Reisæter[3], J. Rørvik[4], P. Steenbergen[2], L.P. Muren[1]

[1]Aarhus University Hospital, Dept of Medical Physics, Aarhus, Denmark

[2]Netherlands Cancer Institute, Dept of Radiation Oncology, Amsterdam, The Netherlands

[3]University of Bergen, Dept of Clinical Medicine, Bergen, Norway

[4]Haukeland University Hospital, Dept of Radiology, Bergen, Norway

Purpose/Objective: Tumour control probability (TCP) models may be useful for evaluation and optimisation of radiotherapy (RT), in particular in dose escalation/painting strategies. Most TCP models apply homogeneous values of the involved parameters such as the initial tumour cell density or the involved radiobiological parameters. However, functional imaging techniques may provide patient-specific information that could be taken advantage of in TCP modelling. Focusing on RT of prostate cancer, the aim of this study was to develop a method for individualising TCP models based on tumour cell density distributions estimated from magnetic resonance imaging-based apparent diffusion coefficient (ADC) maps.

Materials and Methods: The TCP models were based on linear-quadratic cell survival curves, while also including terms such as treatment time (i.e. repopulation, with an effective doubling time of 28 days), cell repair (with a repair half time of 5 h) as well as a variation of the radiobiological parameters between sub-populations (SD of α and ß of 15%). Using ADC maps in a series of 10 prostate cancer patients, the initial number of clonogens in each voxel ($N_{0,i} = r_i \cdot V_{voxel}$) was estimated using two different approaches for the relation between ADC values and cell density, a linear (LIN) and a sigmoid (SIGMOID) relation; each of the relations were used either in the index tumour or for the whole prostate (Table 1). The linear relation was derived from the results of Gibbs et al. 2009 while the SIGMOID relation modulated the cell density between two constant values, $1.9 \cdot 10^5$ cell/cm^3 (Walsh and van der Putten 2013) and 10^7 cell/cm^3 (Søvik et al. 2007). TCP calculations were also performed using these two uniform densities for the whole prostate tissue. All TCP calculations were performed assuming an α/ß = 1.93 Gy from a recent meta-analysis (Vogelius and Bentzen 2013) and α = 0.18 Gy^{-1} (consistent with clinical outcomes in the same meta-analysis).

Results:

Table 1. Volume and ADC values for the prostate and index lesion, and initial number of clonogens for the different approaches of cell density.

	Median	Range
Prostate Volume (cm^3)	40.4	32.7 – 83.5
Index Volume (cm^3)	2.1	0.3 – 17.0
ADC within Index (mm^2/ms)	0.9	0.3 – 2.3
ADC outside of Index (mm^2/ms)	1.3	0 – 2.9
$N_{0,i}$ LIN Prostate (10^8 cells)	291.7	206.1 – 618.1
$N_{0,i}$ LIN Index (10^8 cells)	21.5	2.8 – 172.9
$N_{0,i}$ SIGMOID Prostate (10^8 cells)	3.6	2.5 – 7.0
$N_{0,i}$ SIGMOID Index (10^8 cells)	0.6	0.4 – 2.0
$N_{0,i}$ ρ=1.9·10^5 (10^8 cells)	0.1	0.1 – 0.2
$N_{0,i}$ ρ=10^7 (10^8 cells)	4.0	3.3 – 8.4

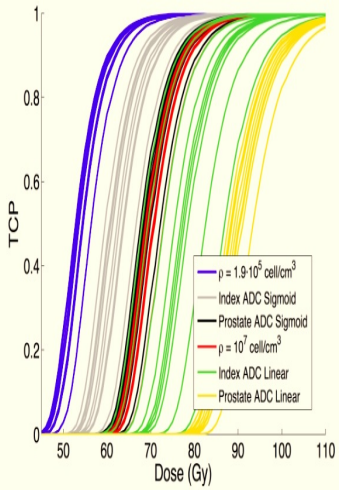

Figure 1. TCP curves using the LQ model with the modifying terms, computed for the six different approaches of the voxel cell density: two constant cell density (blue and red curves), two assuming a sigmoid relation between ADC and cell density (gray and black) and two assuming linear relation between the ADC values and cell density (green and yellow)

Overall, TCP curves based on ADC maps showed larger differences between individuals than those assuming a uniform cell density. Using the SIGMOID relation for the index lesion, the range of D50% (the dose required to reach 50% TCP) was 9.6 Gy, compared to 5.3 Gy using a constant density for the entire prostate of 107 cells/cm3 (Fig. 1). The TCP curves found using the SIGMOID relation for the whole prostate were very close to those found using a constant cell density of 107 cells/cm3. The two linear approaches gave lower TCP values (for the same dose) than either of these approaches.

Conclusions: This study has showed how ADC maps can be used to estimate voxel cell density to allow for an individualised TCP model for use in RT of prostate cancer. The individualised, voxel-based cell density distributions resulted in TCP curves with a larger range in $D_{50\%}$ compared with the TCP models based on uniform cell density distributions.

PO-0906

Is the anal sphincter a key structure for gastrointestinal toxicity in prostate cancer radiotherapy?